J Mater Sci: Mater Med (2015) 26:259
DOI 10.1007/s10856-015-5594-0

Original Research

Porous titanium and Ti–35Nb alloy: effects on gene expression of osteoblastic cells derived from human alveolar bone

Renata Falchete do Prado[1] · Sylvia Bicalho Rabêlo[1] · Dennia Perez de Andrade[1] · Rodrigo Dias Nascimento[1] · Vinicius André Rodrigues Henriques[2] · Yasmin Rodarte Carvalho[1] · Carlos Alberto Alves Cairo[2] · Luana Marotta Reis de Vasconcellos[1]

Received: 2 June 2015 / Accepted: 26 September 2015 / Published online: 8 October 2015

Abstract Tests on titanium alloys that possess low elastic modulus, corrosion resistance and minimal potential toxicity are ongoing. This study aimed to evaluate the behavior of human osteoblastic cells cultured on dense and porous Titanium (Ti) samples comparing to dense and porous Ti–35 Niobium (Ti–35Nb) samples, using gene expression analysis. Scanning electronic microscopy confirmed surface porosity and pore interconnectivity and X-ray diffraction showed titanium beta-phase stabilization in Ti–35Nb alloy. There were no differences in expression of transforming growth factor-β, integrin-β1, alkaline phosphatase, osteopontin, macrophage colony stimulating factor, prostaglandin E synthase, and apolipoprotein E regarding the type of alloy, porosity and experimental period. The experimental period was a significant factor for the markers: bone sialoprotein II and interleukin 6, with expression increasing over time. Porosity diminished Runt-related transcription factor-2 (Runx-2) expression. Cells adhering to the Ti–35Nb alloy showed statistically similar expression to those adhering to commercially pure Ti grade II, for all the markers tested. In conclusion, the molecular mechanisms of interaction between human osteoblasts and the Ti–35Nb alloy follow the principal routes of osseointegration of commercially pure Ti grade II. Porosity impaired the route of transcription factor Runx-2.

✉ Renata Falchete do Prado
renatafalchete@hotmail.com

[1] Institute of Science and Technology, São Paulo State University, Av. Engenheiro Francisco José Longo, 777, São José dos Campos, São Paulo 12245-000, Brazil

[2] Material Division, Air and Space Institute, General Command of Aerospace Technology, São José dos Campos, Praça Mal. do Ar Eduardo Gomes, 14, São José dos Campos, São Paulo 12904-000, Brazil

1 Introduction

Titanium is a key biomaterial, applied in medical science, presenting good mechanical properties and excellent bone-contact biocompatility. Although its elastic modulus (110 GPa) [1] can cause "stress shielding" or "blinding", a phenomenon resulting from the charge transfer resistance of an implant into the surrounding bone. The Ti–6Al–4V alloy is the most widely used in the manufacture of implants [2]. The elastic modulus of this alloy (110–114 GPa) is higher than the elastic modulus of bone [3, 4], causing stress shielding.

This phenomenon can cause bone resorption around the implant and its eventual failure. Thus, in addition to being biocompatible, bone replacement materials must also be mechanically compatible [2, 5, 6]. To address this, corrosion resistant; low modulus alloys, possessing no toxic potential, have been widely developed since the 1990s [6, 7].

One of the properties that determine the elastic modulus of a material is the structural phase of the metal. At room temperature, titanium occurs in α phase, with a compact hexagonal crystal structure, which can be allotropically transformed into the β phase, a body-centered cubic structure. The addition of chemical elements to produce an alloy aims to maintain the α or β phase, but despite this, many titanium alloys exhibit both phases [1].

Among inert metals, niobium is the main stabilizer of the β phase of titanium and when alloyed to it, between 10 and 20 % or 35–50 % weight, the alloy presents inferior elastic modulus (less than 85 GPa) [8, 9].

The titanium–35 niobium (Ti–35Nb) shows predominance of β phase, elastic modulus of approximately 80 GPa and tensile strength of 600 MPa [10]. These properties, together with its high bone-contact biocompatibility and resistance to corrosion, characterize it as a material with potential biomedical applications [11].

Composition, surface energy, roughness and topography control the events at the bone-implant interface during osseointegration [12, 13]. It is known that greater bone fixation occurs when the implant surface is rough or porous compared with a smooth surface [14, 15]. The osseointegration of porous titanium is due to bone growth into the pores, denominated "bone ingrowth" [15]. This results in greater surface contact at the bone-implant interface, leading to improved osseointegration [16].

However, little is known about the effects of topography on the differentiation of bone precursor cells [17]. Topography can enhance osteoblast differentiation by regulating transcription activity or gene regulation of key osteogenic factors. This probably occurs due to the change in shape of osteoblasts when these cells interact with the implant surface microtopography [18]. To understand why porous titanium implants promote better osseointegration, studies that evaluate in vitro osteoblast responses can be used [19].

In the present study, a Ti–35Nb alloy porous scaffold was prepared, by powder metallurgy, through a space holder sintering method. This is an useful technology for the production of complicated shape such as interconnectivity pores [16, 20, 21]. Thus, the purpose of this study was to evaluate the in vitro behavior of human osteoblastic cells cultured on dense and porous titanium scaffolds and compare with dense and porous scaffold of titanium–35 niobium alloy (Ti–35Nb) by analyzing the gene expression. The characterization of samples was performed using scanning electron microscopy (SEM), energy dispersive spectroscopy (EDS) and X-ray diffraction (XRD). The mechanical property was analyzed by Young elastic modulus.

2 Materials and methods

2.1 Sample fabrication

Five groups were delineated, as follows: Group 1-calibrator (polystyrene plate well); Group 2-dense pure titanium grade II samples; Group 3-porous pure titanium grade II samples; Group 4-dense Ti–35Nb alloy samples; and Group 5-porous Ti–35Nb alloy samples.

Elemental metal powder of pure Ti grade II with (purity ≥99.5 %), was prepared by hydrogenation and dehydrogenation (HDDH), and Nb (purity 99 %) powder was obtained using the same route. The characteristics of the powders used in the Ti–35Nb alloy preparation (previously described Santos et al. 2008) were: Ti mean particle size (μm) 3.28, Nb mean particle size (μm) 10.22, for both, particle morphology was angular, the process for powder production was hydriding, wherein Ti melting point was 1670 °C; Nb 2468 °C, and Ti hydriding temperature was 500 °C and Nb 800 °C. The samples were prepared by powder metallurgy, developed at the Materials Division of the Aeronautics and Space Institute (IAE) of the General Command of Aerospace Technology, São José dos Campos, SP, Brazil.

The Ti–35Nb alloy was fabricated using the element-powder sintering technique, proposed by Santos [10]. Ti and Nb powders were used in a hydrogenated state by adding hydrogen during the process, in order to activate sintering and to reduce costs. The precursor powders were weighed on an analytical balance to adjust the stoichiometry of the alloy. The mixture was placed in a rotary agitator, encased with titanium plates and filled with titanium balls, for 30 min.

The samples were disc-shaped scaffolds, fabricated using a steel mold: 12 mm in diameter and 5 mm in height. For dense samples, the pure Ti grade II or Ti–35Nb powder was inserted into the mold and the unit was subjected to compaction in a uniaxial press (Carver Laboratory Press Wabash, England) at 0.7 tons, and then cold compaction in an isostatic press (Paul Weber Maschinen, Apparaebau Fuhrbachstrabe Remshalden Grunbach) at 200 MPa. Next, they were sintered in a vacuum oven (Thermal Technology, California, USA) at 7.10 torr, with a heating rate of 10 °C/min, reaching a threshold of 1200 °C for 1 h.

Porous samples were obtained mixing pure Ti grade II powder or Ti–35Nb with an organic additive: urea, $(NH_2)_2CO$ (JT Baker Phillipsburg, USA), used as a spacer with particles ranging from 177 to 250 μm. Following, the powders were mixed for 1 h by a mechanical V mixer (Treu Rio de Janeiro, Brazil). The samples were compacted as per the dense samples. To remove the urea, the samples were incubated in a vacuum oven (Marconi, Piracicaba, São Paulo, Brazil), at 200 °C for 2 h. The temperature of 200 °C, used for evaporation of urea was based in previous thermogravimetric analysis.

To clean the samples, they were immersed in neutral detergent, distilled water, acetone and distilled water, each one during 20 min in ultrasound. Then, samples were dry in incubator and sterilized prior to contact with the cell culture.

2.2 Samples characterization

SEM (Carl Zeiss, Brazil; Microanalysis Group, Oxford, England) equipped with energy-dispersive spectrometer

(EDS) (Oxford with Detector Model 7059) were used to characterize the microtopography (surface morphology, pore size and interconnectivity of the pores in the porous sample) and elements present in samples.

Five randomly distributed fields on the surface of five samples of each group were photographed at ×100 magnification (25 fields per group). Image J (NHI) was used for the metallographic analysis of the porous size. Data were submitted to statistic test.

The structure was determined by XRD. Angle profiles were recorded at a scan speed of 0.42°/s, using a diffractometer (PANalytical, Xpert, Pro MPD 3060).

The porosity (fraction of the pore volume obtained by gravimetric analysis) of the porous samples was determined by Eq. [1] where ρ and ρ_s represent the apparent density of the sintered porous sample and the theoretical density of solid metal, respectively.

Dense samples were measured and weighed, and based upon the formula density = mass divided by the volume, theoretical density was obtained for titanium = 4.4 g/cm^3 and Ti–35Nb alloy = 4.9 g/cm^3. The apparent density of the porous sample was determined from its weight and dimensional measurements.

$$p = [1 - \rho/\rho_s] \text{ x } 100\ \% \quad (1)$$

2.3 Measurement of mechanical properties on porous Ti–35Nb

Compressive strength was obtained by unidirectional compression in three dense and three porous cylindrical samples, of each material, using universal testing equipment (810 Material Test System MTS Systems Corporation Eden Prairie, MN, USA) at cross-head speed of 0.5 mm/min. This test was performed using ASTM E09-09 standard. Young modulus [E] was acquired using the following formula: $E = \sigma/\varepsilon$, were σ is tensile stress and ε is extensional strain. The compression strength and elastic modulus of samples (different materials, dense and porous) were analyzed and compared.

2.4 Isolation of human osteoblastic cell and development of osteogenic cultures

This study was approved by the Human Research Ethics Committee of the Institute of Science and Technology, São Paulo State University (UNESP)—Univ Estadual Paulista, (029/2010-PH/CEP) and was conducted after donors signed a term of free informed consent. All work was conducted using material provided by three normal donors who were submitted to surgeries in which bone fragments were naturally removed. Donors were two men and one woman. Mean aged at 40 years. Two had interradicular septum removed after tooth extraction because of dental caries and one donor had ridge regularization for implant protocol.

Osteogenic cells were isolated by sequential enzymatic digestion of fragments of human alveolar bone tissue with collagenase type II (Gibco-Life), as previously described [22, 23]. Next, the bone explants were maintained in a culture flask containing alpha modified minimum essential medium (α-MEM), supplemented with 10 % fetal bovine serum, 50 μg/mL gentamicin, 0.3 μg/mL of fungizone, 10^{-7} M dexamethasone (Sigma), 5 mg/mL ascorbic acid and 7 mM beta-glycerophosphate (Sigma), in a CO_2 chamber at 37 °C.

The medium was changed every 72 h for approximately 15 days, when cell confluence occurred. On the day of plating, cells were enzymatically removed with a solution containing 0.25 % trypsin, collagenase II and 1 mM EDTA; counted in a Neubauer chamber and plated on the sterile samples enclosed in 24-well polystyrene plates at a density of 2×10^4 cells/well with same supplemented medium above.

2.5 Selection of genes for the relative quantification by reverse-transcriptase PCR in real time

The expression of the following genes was evaluated at 7 and 14 days. Profile of genes involved in osteogenesis namely alkaline phosphatase (ALP), type I collagen, osteopontin, osteocalcin, osteonectin and bone sialoprotein (BSP) was analyzed. The signaling activity of transforming growth factor-β is frequently manifested by the transcription factor Runx-2, while Osterix play a key role downstream of Runx-2, which is associated with differentiation of osteoblasts. Thus, their expressions were accessed. Integrin and its associated molecules play one of the most important roles in the interaction of cells with any substratum, so integrin β1 was evaluated.

Interleukin is predominantly activated in the acute reaction phase and its high levels suggest early transplantation—related complications and Prostaglandin E2 synthase is involve in inflammatory response. Macrophage Colony stimulating factor is related to reabsorption phenomenon and apolipoprotein E blocks osteoclasts differentiation, apparently having antagonistic effects. These markers may be involved in implant loss.

2.6 Total RNA isolation and purification

Total RNA extraction was performed on cells adhering to the Ti and Ti–35Nb scaffolds using TRIzol reagent® (Ambion Life Technologies Corp., Van Allen Way, Carlsbad, CA, USA), in accordance with the manufacturer's instructions. The concentration and purity of the

RNA samples were determined by optical density in a Nano Drop 2000 spectrophotometer (Thermo Fisher Scientific Inc., Wilmington, DE, USA). Next, the quality and integrity of the RNA was assessed by agarose gel electrophoresis.

The biological triplicate (three bone donors) that came into contact with samples from each group was used to create an RNA pool. Thus, following the union of the corresponding experimental groups, the RNA was quantified again prior to the next step.

RNA was purified by Deoxyribonuclease I, Amplification Grade (Invitrogen, Life Technologies Corp., Van Allen Way, Carlsbad, CA, USA), in accordance with the manufacturer's instructions.

2.7 cDNA synthesis and RT-PCR

Complementary deoxyribonucleic acid (cDNA) was synthesized using 500 ng RNA through a reverse transcription reaction using a high-capacity cDNA reverse transcription kit (SuperScript® III First-Strand Synthesis SuperMix—Invitrogen), according to the instructions of manufacturer. cDNA was stored at −20 °C.

The cDNA was used in the Line-Gene K Real-Time PCR Detection System (Bioer Technology Hi-tech, Binjiang District, Hangzhou, People's Republic of China), and stained with the Platinum® SYBR® Green qPCR SuperMix-UDG system (Invitrogen). Specific primers and 2 μL of cDNA were used in each reaction. The reactions were performed in triplicate and the primers used are listed in Table 1. The RT-PCR conditions were standardized using melting and efficiency curves based on the suggestions of the manufacturer of the SYBR® Green, and primer melting temperatures using a calibrator sample. Efficiencies between 85 and 105 % and correlation coefficients of 0.995 or greater were accepted.

The samples were submitted to RT-PCR for beta-actin, HPRT1 and GAPDH. The site http://www.leonxie.com/referencegene.php?type=reference# was accessed and determined beta-actin as preferred reference gene according ΔC_t method, Normfinder and Genorm. Relative quantification was performed according to Livak & Schmittgen [24].

2.8 Statistical analysis

Statistical comparison of the porosity obtained by the geometric method and by metallography was performed using the Student t test. Gene expression of the key osteoblast markers was compared using ANOVA up to-three-way (time and alloy and porosity), followed by complementary Turkey's multiple comparison test when appropriated. A value of $P < 0.05$ was considered significant.

3 Results

3.1 Structural analysis

After a vacuum high temperature sintering, both titanium and titanium-niobium formed a structure with a rough surface. The addition of urea to powder resulted in porous structure with rough surface. Pore morphology, distribution and interconnectivity were demonstrated in images obtained by SEM. Pores of varying sizes were detected and three-dimensional connectivity was observed between them. In addition to large pores (macropores), under higher magnification, the SEM images revealed the existence of many micropores on the rough surfaces of the scaffolds.

EDS data showed that the main element for the groups made of commercially pure Ti grade II was titanium (strongest signal at 4.5 keV) and the samples made with the Ti–35Nb alloy presented niobium (strongest signal at 2.2 keV) and titanium as main components.

Figure 1 shows the XRD spectra of the sintered pure grade II-Ti and Ti–35Nb alloys. All the sintered Ti–35Nb alloy samples were composed of α-phase and β-phase, while, only analysis by XRD performed on the sample of pure titanium showed only the α-phase. In the samples of Ti–35Nb, the primary β-phase peak is superimposed on the α-phase peak in 2θ equal to 38.4°. The identification of β-phase (obtained from the dissolution of the Nb particles) was confirmed by the isolated peak in 2θ equal to 55.5°.

The majority of pores measured between 300 and 100 μm (mean of 193.85 μm). A statistical analysis revealed that the porous pure Ti ranged between 76.50 and 534.72 μm (mean 226.46 μm), and porous Ti–35Nb showed pore size between 38.98 and 387.11 μm (mean 161.23 μm), been statistically difference. The porous Ti and Ti–35Nb samples showed mean of porosity of 33.79 ± 1.69 and 54.5 ± 5.4 %, respectively.

The mean of Young modulus obtained in Ti dense samples was 47.71(±7.18) GPa. Titanium porous specimens demonstrated elastic modulus of 18.30 (± 8.05) GPa. The value of elastic modulus of the dense and porous titanium-niobium alloy was of 25.82 (±11.03) GPa and 6.44 (±1.62) GPa respectively. Groups were statistically different with $P < 0.05$.

3.2 Cell analysis

SEM analysis of scaffold after 7 and 14 days in cell culture showed adhering cells to Ti and Ti–35Nb surfaces,

Table 1 Description of the primers

Gene	Primers sense/antisense	Primer melting temperature (°C)	Base pairs	FASTA PUBMED References
Beta-actina	AAACTGGAACGGTGAAGGTG	55.4	206	NM_001101.3
	GTGGACTTGGGAGAGGACTG	57.1		
GAPDH	GAGTCAACGGATTTGGTCGT	52.5	201	NM_002046.6
	TGGGATTTCCATTGATGAAC	48.7		
HPRT	TGCTCGAGATGTTGATGA	46.5	192	NM_000192.2
	TCCCCTGTTGACTGGTCATT	52.5		
Alkaline phosphatase	CCACGTCTTCACATTTGGTG	54.2	196	NM_000478.4
	AGACTGCGCCTGGTAGTTGT	58.8		
Osteocalcin	AGCAGAGCGACACCCTAGAC	57.5	194	NM_001199662.1
	GGCAGCGAGGTAGTGAAGAG	58.8		
Osteopontin	AGACACATATGATGGCCGAGG	56.7	154	NM_001251830.1
	GGCCTTGTATGCACCATTCAA	55.9		
Bone sialoprotein II	GCAGTAGTGACTCATCCGAAGAA	56.4	121	NM_004967.3
	GCCTCAGAGTCTTCATCTTCATTC	55.2		
Osteonectin	ACTGGCTCAAGAACGTCCTGGT	60.7	97	NM_003118.3
	TCATGGATCTTCTTCACCCGC	57.1		
Collagen-1	ACAGCCGCTTCACCTACAGC	60.1	85	NM_000088.3
	GTTTTGTATTCAATCACTGTCTTGCC	55.0		
Runx2	GAACTGGGCCCTTTTTCAGA	55.3	208	NM_001015051
	CACTCTGGCTTTGGGAAGAG	55.6		
Osterix	GCCATTCTGGGCTTGGGTATC	58.3	129	NM_001173467.1
	GAAGCCGGAGTGCAGGTATCA	59.2		
Prostaglandin E2 synthase	GAAGAAGGCCTTTGCCAA	53.2	200	NM_004878.4
	GGAAGACCAGGAAGTGCA	54.6		
TFG-B	TTTGATGTCACCGGAGTTGTG	55.4	63	NM_000660.4
	GCGAAAGCCCTCAATTTCC	54.6		
Integrin B-1	TTCTTCCTGGACTATTGAAAT	48.9	100	NM_002211.3
	AGAAACTCTCATCATGCTCATT	51.9		
Interleukin 6	CAATAACCACCCCTGAC	49.8	84	NM_000600.3
	TTGTCATGTCCTGCAGCCACT	59.3		
M-CSF	GAGCTGCTTCACCAAGGATTATG	55.9	92	NM_172211.3
	TCTTGACCTTCTCCAGCAACTG	56.9		
Apolipoprotein E	CACTGTCTGAGCAGGTGCAG	58.2	112	NM_000041.2
	TCCAGTTCCGATTTGTAGGC	54.8		

Sense and antisense sequences, their melting temperatures, the size of the amplified, and reference

including entering in macropores, with long and numerous filopodia assuming star shape aspect.

3.3 Real-time qPCR

The expression of TGF-β, integrin-β1, ALP, osteopontin, M-CSF, prostaglandin E2 synthase and apolipoprotein E showed no statistically significant difference between groups, independently of composition, topography and time (Figs. 2, 3, 4).

The factor composition was insignificant, since cells adhering to the Ti–35Nb alloy showed similar gene expression to pure Ti grade II for all genes (Figs. 2, 3, 4). However, collagen 1, Osteonectin, Osteocalcin and Osterix showed variable expression between experimental groups (Ti and Ti–35Nb) when comparing to calibrator group: cells plated on polystyrene well (Fig. 2, 3).

The factor topography, after tested by ANOVA showed that porous groups showed significant reduced expression of Runx-2 when compared to dense groups (Fig. 3).

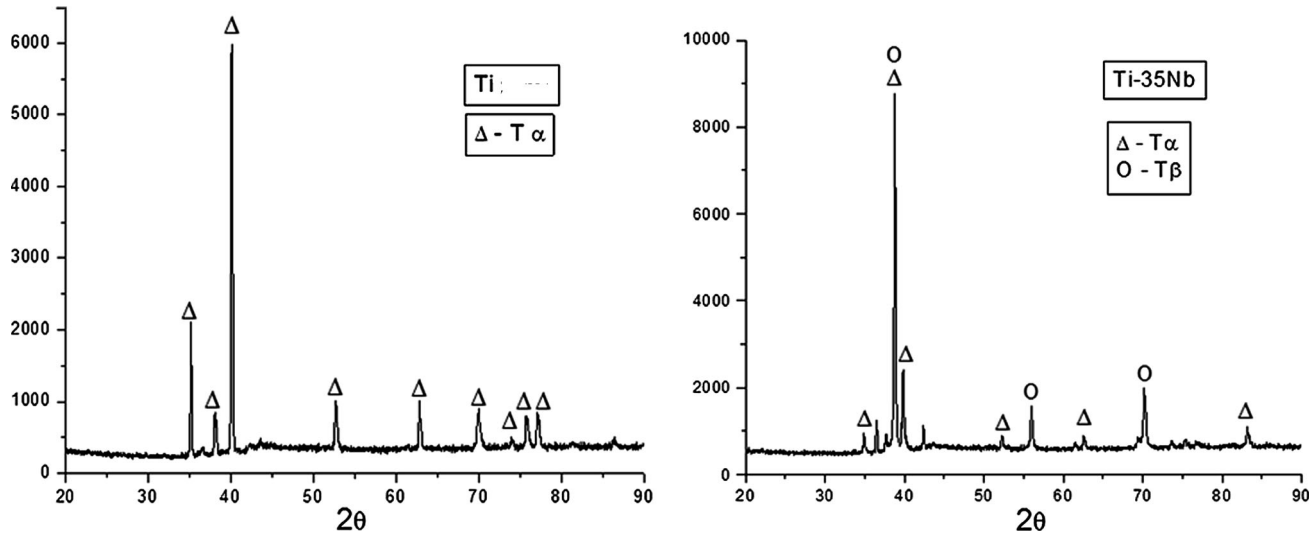

Fig. 1 X-ray diffraction. XRD patterns of pure Ti scaffolds obtained by powder metallurgy after sintering at 1400 °C for 1 h, in which only α-phase was detected and XRD patterns of Ti–35Nb scaffolds obtained by powder metallurgy after sintering at 1400 °C for 1 h in which α-phase (Tα) and β-phase (Tβ) were detected

The factor time (7 or 14 days) was significant for the markers BSP II (BSP II—Fig. 2) and interleukin 6 (Fig. 4). Their expression increased over time.

4 Discussion

Titanium and its alloys are accepted in medical application because provide high strength to weight ratios, good fatigue strength and increased corrosion resistance compared with other materials [3]. However, in applied biomaterials the surface features such as: chemical composition, roughness, internal pore size and porosity also must be considered [25]. These characteristics have direct effects on osteoblast migration, attachment, proliferation and osteoblastic differentiation [26].

This study demonstrated that Ti–35Nb is a suitable material for biomedical applications, since genic data, covering differentiation, adhesion, inflammatory and cellular signaling functions, was similar to gold standard: pure titanium. Besides that, Ti–35Nb revealed advantageous mechanical properties with lower Young elastic modulus, regardless of the topography. The porosity diminished elastic modulus, been a positive modification independently material composition.

Material Young elastic modulus is a critical property in longevity of endosseous loading implants [27]. This mechanical property may be changed according composition of material [28] or topography containing pores [29]. In this study, the porosity indeed improved alloy property, since Ti–35Nb alloy exhibited the lowest elastic modulus, in line with previous study [25]. In the present study, the average of elastic modulus in porous and dense Ti–35Nb samples were comparable to that found in natural bone 10–20GPa [30]; this aspect results in more favorable local mechanical environment between bone and implants [16].

The influence of the chemical composition of the material in the elastic modulus is related to the stabilization of the β phase of titanium, which can be obtained by the addition of various metal elements such as niobium, tantalum and zirconium [31]. This property of Nb was detected by XRD analysis results of this study. Moreover, Ti–Nb alloys are considered viable alternatives being less toxic than traditional alloy Ti–6Al–4V [32] with biocompatibility similar to commercially pure titanium [33], result also found in this study according genic expression.

The porosity aim to mimic the natural bone [34] and additionally decrease elastic modulus [29]. In vivo, promotes tissue ingrowth [16] and in vitro, osteoblastic differentiation [26]. The architecture of the porous surface can be composed of isolated pores obtained by chemical treatments [35] and sandblasting [36] or interconnected, made by specific techniques, including the powder metallurgy [16, 25, 29]. In powder metallurgy the interconnected macropores can be obtained by the decomposition of urea particles which were used as spacer. On the other hand, the micropores were obtained by partial sintering of the metal powders, but it also help to interconnect pores. The interconnectivity facilitates distribution of nutrients by neoformed blood vessels.

Porosity and pore diameter are important parameters in biological porous materials [25]. However, there is no consensus for optimal pore size and porosity [37, 38]. In this study the pore size (>100 μm) and the porosity, that

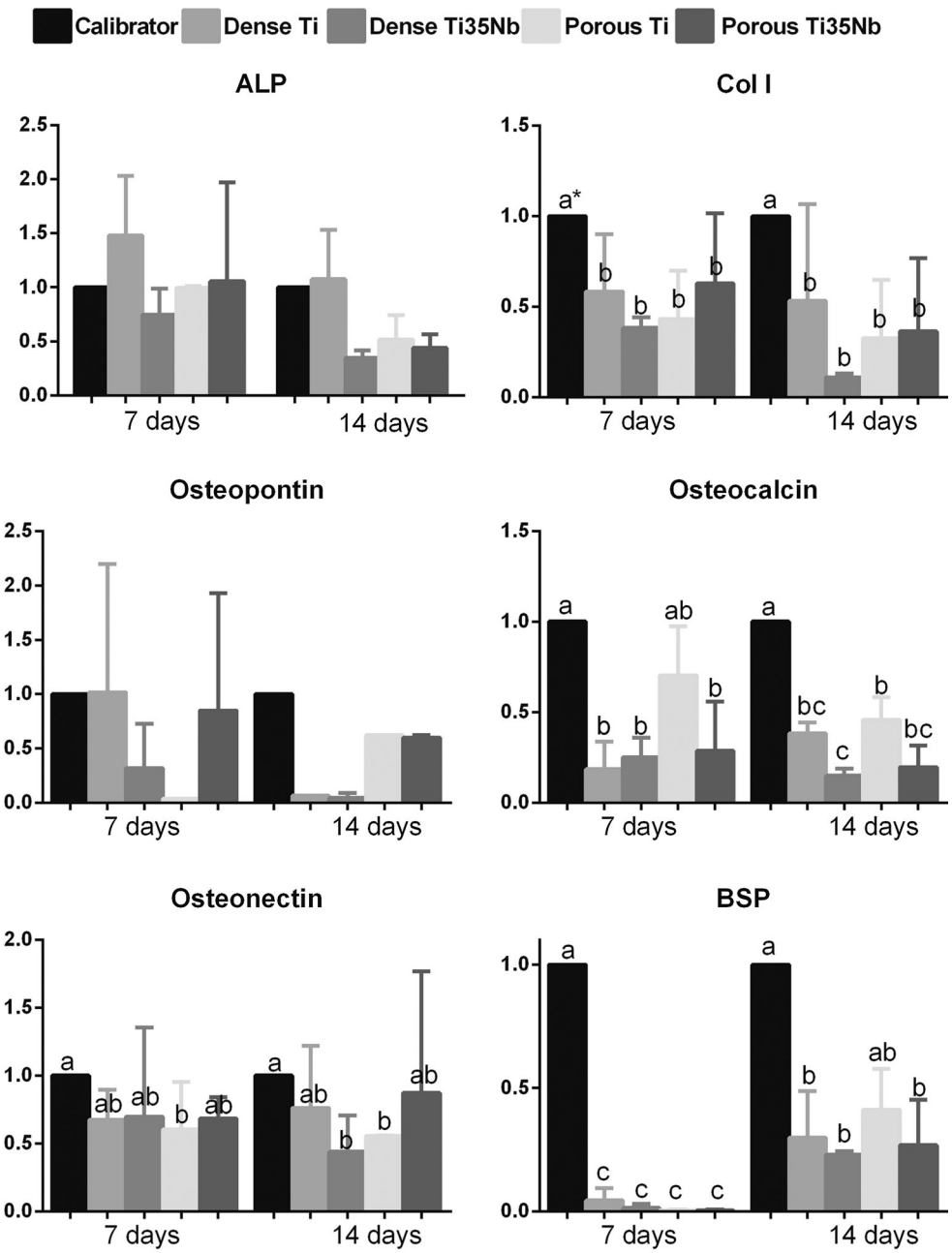

Fig. 2 Data of molecular analysis. Relative quantification of alkaline phosphatase (ALP), collagen I (Col I), osteopontin, osteocalcin, osteonectin and bone sialoprotein II (BSP) after 7 and 14 days of contact with each group. Tukey test results are seen in *superscript letters* when any factor was significant after ANOVA-three way analysis. *Error bar* represents standard deviation

ranged between materials, complied with requirements for porous biomaterials implants [29, 38], since their average are considered appropriated to promote cell proliferation [39]. Then, the porosity and pore size of experimental samples produced in this study may be hopeful for the ingrowth of new bone in vivo.

Several studies use different cell lines, for example MG63 immortalized human osteossarcoma cells [40], MC3T3E1 osteoblast like cells [27, 33], saos-2 [38] to assess osteoblast behavior or differentiation in contact to titanium, and, most of them, reported better results in experimental groups [surfaces modifications or alloys]. According, Cooper et al. [41] there is an incomplete pattern of osteoblastic differentiation in immortalized cell lines, justifying some divergent results obtained in this study. Since in the present study, it was used a cell culture model from human explants of alveolar bone, and in most of analysis, there was no significant difference among the

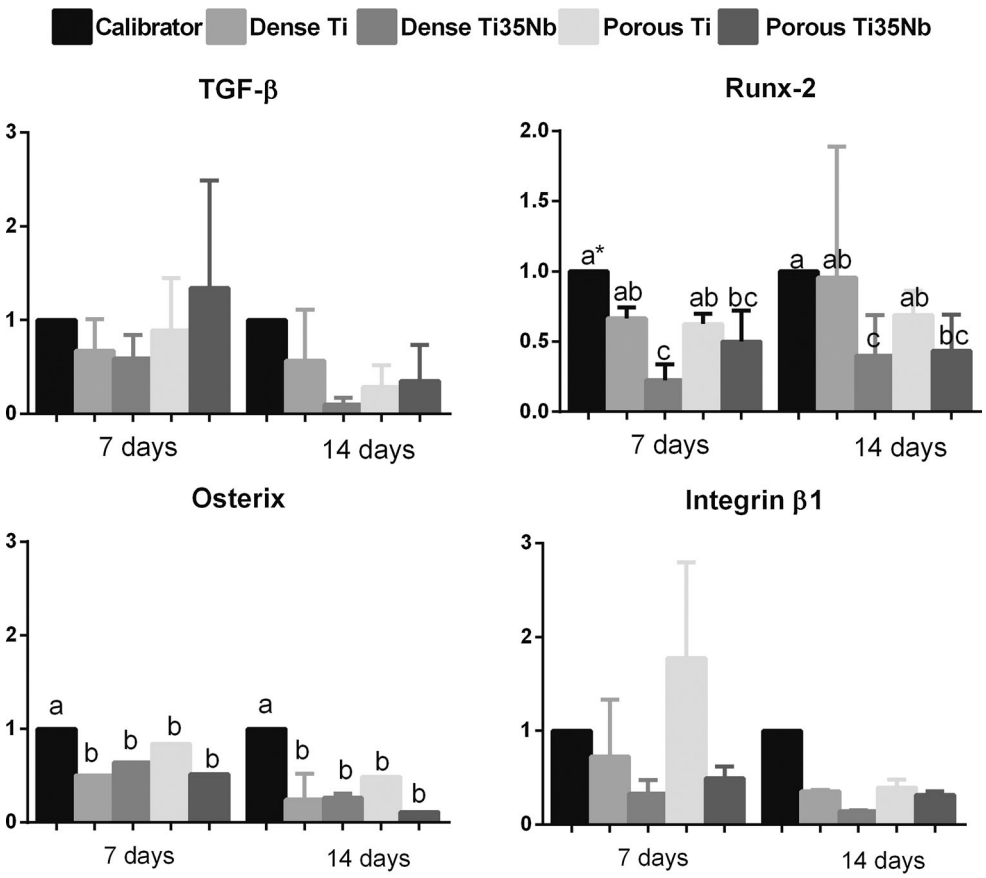

Fig. 3 Data of molecular analysis. Relative quantification of transforming growth factor-β (TGF-β), runt-related transcription factor-2 (Runx-2), osterix and integrin-β1 after 7 and 14 days of contact with each group. Tukey test results are seen in *superscript letters* when any factor was significant after ANOVA-three way analysis. *Error bar* represents Standard Deviation

experimental groups, independently of chemical composition or topography surface. In line with this observation, previous researchers using primary or subcultured cell also did not found improved osteoblastic activity in experimental Ti modified surfaces [42, 43].

The expression of genes and proteins involved in bone growth and repair are valuable markers for demonstrating the osteoblast phenotype in vitro. Studies of variable composition and surface topographies of new developed material investigate gene expression of osteoblasts to prove their biocompatibility [33, 35, 37, 44].

Osteoblasts express encoding genes of bone matrix proteins, ALP and parathormone receptors. Type I collagen comprises of approximately 90 % of bone organic matrix. Noncollagenous bone proteins comprise osteocalcin, osteopontin, osteonectin and BSP. Together, these proteins orchestrate calcium binding by regulating the deposition of hydroxyapatite crystals, their arrangement and the size of crystals perceived in the mineralized bone matrix [45]. During osteoblast differentiation and maturation, collagen type I production and ALP enzymatic activity are followed by the secretion of RGD glycoproteins (involved in the ability of the extracellular protein to bind to integrin cell surface receptors), such as BSP and osteopontin. Finally the most specific marker of mature osteoblasts is synthetized: osteocalcin [46]. In this study, Col I, ALP, integrin, OP, BSP, osterix and OC showed, mostly of analysis, similar gene expression patterns, independently of chemical composition or topography samples. Corroborating to these observations, Ferraz et al. [42] did not observed positive effect of modify Ti surfaces in gene expression of key osteoblast markers, unlike of previous study that have demonstrated difference in expression in some of these genes on surfaces with different topography or composition [33].

Runx-2 and osterix are the major osteoblast transcription factors involved in osteoblast differentiation and bone formation [35]. The Runx-2 expression was lower in most of porous groups, however, statistically significant only when comparing pure Ti, similar to previous data from Pereira et al. 2013 [47] at 7 days of experiment. Previous study [35, 47] found conflicting results of Runx-2 level. Thus, it is necessary to investigate the role of surface topography on the expression of Runx 2.

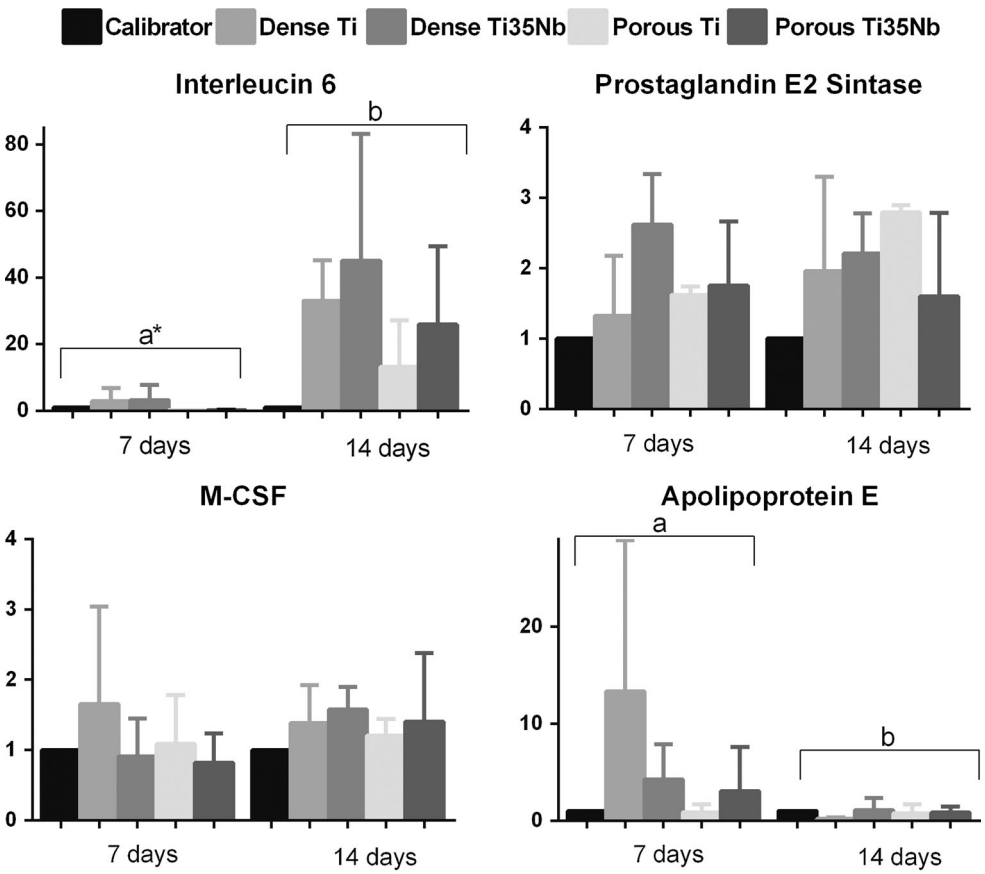

Fig. 4 Data of molecular analysis. Relative quantification of interleukin 6, prostaglandin E2 synthase, macrophage colony stimulating factor (M-CSF) and apolipoprotein, after 7 and 14 days of contact with each group. Tukey test results are seen in *superscript letters* when any factor was significant after ANOVA-three way analysis. *Error bar* represents standard deviation

Osterix has correlation with integrin expression, since osterix is a transcription factor involved in the metabolic pathway of cell adhesion through integrins, maintaining continual osteogenic differentiation, in contrast with chondrogenic differentiation [18]. This correlation was observed in this study indicating osteoblastic differentiation. Integrin-β1 expression was similar in all groups as observed by Sista et al. 2013 [33]. Additionally osterix and osteocalcin, which is a marker of fully matured osteoblasts [46], exhibited similar patterns of expression, both upregulated on dense Ti–35Nb samples, but without statically difference with others groups. Literature presents conflicting results on the osteocalcin expression values in control and experimental surfaces [33, 42, 47].

Osteonectin, osteopontin and bone sialoprotin are specific markers of extracellular matrix in the period of mineralization [45]. We analyzed gene expression of these osteogenic markers and, in some comparisons; they exhibited higher values in Ti–35Nb samples. Osteonectin expression was higher in cells adhered to porous Ti–35Nb and dense pure Ti when compared with the others groups, but not statistically different. These results are similar to those previously reported [33], in which the niobium alloy group presented higher levels of osteonectin. Osteopontin expression was more favorable in both Ti–35Nb samples, at 14 days, and suggests a more mature osteoblastic phenotype in this samples, as noticed in previous articles [33, 48].

Interesting, Pereira et al. [47] and Sista et al. [33], also observed early expression osteopontin in short time in some samples, as we verified the expression higher at 7 days for porous Ti–35Nb samples when compared at 14 days. Pereira et al. [47] suggested that this early enhanced extracellular osteopontin is because an enhanced adsorption of the protein, and not because of a higher osteoblastic activity.

The expression BSP showed a significant increase in expression over the 14 days of culture for all groups, suggesting that bone cells initiated the extracellular matrix production for all surfaces tested. At 14 days the single group with higher expression, similar to calibrator group was the porous Ti–35Nb sample. This increase in BSP expression was also observed in other studies [35, 47]. On the other hand, Sista et al. [33] observed a decrease in the

expression of BSP over time. One hypothesis to explain this divergence, is the different in cultured cells, since this study, did not used immortalized cells, differing from that used by Sista et al. [33]: the MC3T3 lineage.

In addition, to the osteogenic genes markers, Interleukin 6, TGF-B1, prostaglandin E2 synthase, apolipoprotein E and M-CSF were assessed, since they are important in bone metabolism. IL-6, a potent osteoclast activator [49] increased significantly in the all experimental groups at 14 days. It is proposed that there was a differentiation of osteoblastic cells in this period, acquiring attraction activity to osteoclasts.

Evidently, Ti–Nb alloy shows important potential as a biomaterial once molecular data proves that Ti–35Nb alloy is similar to commercially pure titanium. The results for all groups were statistically similar, but numerically higher values were observed for most samples in the Ti–35Nb alloy groups, demonstrating that the chemical composition of the experimental alloy is good for use in biological material. Additionally the architecture of the porous biomaterials may provide a favorable environment for cell growth [26]. This characteristics associated with the best modulus of elasticity presented by the alloy, both in dense and porous samples, became it a promising material to surgery clinic.

5 Conclusions

The molecular mechanisms of interaction between human osteoblasts and the titanium–35 niobium alloy follow the principal routes of osseointegration of commercially pure titanium, and the expression of key markers of cell adhesion and differentiation indicates that the induction of bone matrix synthesis was similar for both. The mechanical properties such as the elastic modulus decrease with chemical composition and porosity of material.

Acknowledgment The authors thank FAPESP [São Paulo State Research Foundation] for the scholarship [PROC 2010/02778-0].

Compliance with ethical standards

Conflict of interest The authors declare no conflict of interest.

References

1. Callister WD, Rethwisch DG. Mechanical properties of metals. Materials science and engineering: an introduction. 8th ed. Danvers: Wiley; 2010.
2. Ning C, Ding D, Dai K, Zhai W, Chen L. The effect of Zr content on the microstructure, mechanical properties and cell attachment of Ti-35Nb-xZr alloys. Biomed Mater. 2010;5(4):045006.
3. Niinomi M. Mechanical properties of biomedical titanium alloys. Mater Sci Eng A. 1998;243(1–2):231–6.
4. Dewidar MM, Yoon HC, Lim JK. Mechanical properties of metals for biomedical applications using powder metallurgy process: a review. Metal Mater Int. 2006;12(3):193–206.
5. Sumner DR, Galante JO. Determinants of stress shielding: design versus materials versus interface. Clin Orthop Relat Res. 1992; 274:202–12.
6. Long M, Rack HJ. Titanium alloys in total joint replacement—a materials science perspective. Biomaterials. 1998;19(18): 1621–39.
7. Niinomi M. Mechanical biocompatibilities of titanium alloys for biomedical applications. J Mech Behav Biomed Mater. 2008;1(1): 30–42.
8. Khan MA, Williams RL, Williams DF. The corrosion behaviour of Ti-6Al-4V, Ti-6Al-7Nb and Ti-13Nb-13Zr in protein solutions. Biomaterials. 1999;20(7):631–7.
9. Davidson JA, Kovacs P, Davidson JA, et al. Biocompatible low modulus titanium alloy for medical implants. United States of America. 1992.
10. Santos DR, Pereira MS, Cairo CAA, Graca MLA, Henriques VAR. Isochronal sintering of the blended elemental Ti-35Nb alloy. Mater Sci Eng A. 2008;472(1–2):193–7.
11. Xiong J, Li Y, Hodgson PD, Wen C. In vitro osteoblast-like cell proliferation on nano-hydroxyapatite coatings with different morphologies on a titanium-niobium shape memory alloy. J Biomed Mater Res A. 2010;95A(3):766–73.
12. Boyan BD, Hummert TW, Dean DD, Schwartz Z. Role of material surfaces in regulating bone and cartilage cell response. Biomaterials. 1996;17(2):137–46.
13. Brunski JB. In vivo bone response to biomechanical loading at the bone/dental-implant interface. Adv Dent Res. 1999;13: 99–119.
14. Pilliar RM, Deporter DA, Watson PA, Todescan R. The endopore implant-enhanced osseointegration with a sintered porous-surfaced design. Oral Health. 1998;88(7):61–4.
15. Deporter DA, Watson PA, Pilliar RM, Chipman ML, Valiquette NA. Histological comparison in the dog of porous-coated vs threaded dental implants. J Dent Res. 1990;69(5):1138–45.
16. Reis de Vasconcellos LM, Oliveira FN, Leite DO, et al. Novel production method of porous surface Ti samples for biomedical application. J Mater Sci Mater Med. 2012;23(2):357–64.
17. Dalby MJ, McCloy D, Robertson M, Wilkinson CDW, Oreffo ROC. Osteoprogenitor response to defined topographies with nanoscale depths. Biomaterials. 2006;27(8):1306–15.
18. Masaki C, Schneider GB, Zaharias R, Seabold D, Stanford C. Effects of implant surface microtopography on osteoblast gene expression. Clin Oral Implants Res. 2005;16(6):650–6.
19. Schwartz Z, Lohmann CH, Vocke AK, et al. Osteoblast response to titanium surface roughness and 1α, 25-(OH) 2D3 is mediated through the mitogen-activated protein kinase (MAPK) pathway. J Biomed Mater Res. 2001;56(3):417–26.
20. Reis de Vasconcellos LM, Moreira Barbara MA, Deco CP, et al. Healing of normal and osteopenic bone with titanium implant and low-level laser therapy (GaAlAs): a histomorphometric study in rats. Laser Med Sci. 2014;29(2):575–80.
21. Vasconcellos LMR, Carvalho YR, Prado RF, et al. Porous titanium by powder metallurgy for biomedical application: characterization, cell citotoxity and in vivo tests of osseointegration. In: Hudak R, Penhaker M, Majernik J, editors. Biomedical engineering: technical applications in medicine. 1st ed. Rijeka: InTech; 2012. p. 47–74.
22. Mailhot JM, Borke JL. An isolation and in vitro culturing method for human intraoral bone cells derived from dental implant preparation sites. Clin Oral Implant Res. 1998;9(1):43–50.
23. Beloti MM, Martins W Jr, Xavier SP, Rosa AL. In vitro osteogenesis induced by cells derived from sites submitted to sinus

grafting with anorganic bovine bone. Clin Oral Implant Res. 2008;19(1):48–54.
24. Livak KJ, Schmittgen TD. Analysis of relative gene expression data using real-time quantitative PCR and the 2(-Delta Delta C(T)) Method. Methods. 2001;25(4):402–8.
25. Xu J, Weng X-J, Wang X, et al. Potential use of porous titanium-niobium alloy in orthopedic implants: preparation and experimental study of its biocompatibility in vitro. Plos One 2013;8(11).
26. Rosa AL, Crippa GE, de Oliveira PT, Taba M Jr, Lefebvre L-P, Beloti MM. Human alveolar bone cell proliferation, expression of osteoblastic phenotype, and matrix mineralization on porous titanium produced by powder metallurgy. Clin Oral Implant Res. 2009;20(5):472–81.
27. Sista S, Wen C, Hodgson PD, Pande G. The influence of surface energy of titanium-zirconium alloy on osteoblast cell functions in vitro. J Biomed Mater Res A. 2011;97A(1):27–36.
28. Navarro M, Michiardi A, Castano O, Planell JA. Biomaterials in orthopaedics. J R Soc Interface. 2008;5(27):1137–58.
29. Hsu HC, Hsu SK, Tsou HK, et al. Fabrication and characterization of porous Ti-7.5Mo alloy scaffolds for biomedical applications. J Mater Sci Mater Med. 2013;24(3):645–57.
30. Choi K, Kuhn JL, Ciarelli MJ, Goldstein SA. The elastic moduli of human subchondral, trabecular, and cortical bone tissue and the size-dependency of cortical bone modulus. J Biomech. 1990;23(11):1103–13.
31. Elmay W, Prima F, Gloriant T, et al. Effects of thermomechanical process on the microstructure and mechanical properties of a fully martensitic titanium-based biomedical alloy. J Mech Behav Biomed Mater. 2013;18:47–56.
32. Challa VS, Mali S, Misra RD. Reduced toxicity and superior cellular response of preosteoblasts to Ti-6Al-7Nb alloy and comparison with Ti-6Al-4V. J Biomed Mater Res A. 2013;101(7):2083–9.
33. Sista S, Wen C, Hodgson PD, Pande G. Expression of cell adhesion and differentiation related genes in MC3T3 osteoblasts plated on titanium alloys: role of surface properties. Mater Sci Eng C Mater Biol Appl. 2013;33(3):1573–82.
34. Lindner M, Bergmann C, Telle R, Fischer H. Calcium phosphate scaffolds mimicking the gradient architecture of native long bones. J Biomed Mater Res A. 2014;102(10):3677–84.
35. Isaac J, Galtayries A, Kizuki T, Kokubo T, Berda A, Sautier JM. Bioengineered titanium surfaces affect the gene-expression and phenotypic response of osteoprogenitor cells derived from mouse calvarial bones. Eur Cell Mater. 2010;20:178–96.
36. Kumar A, Bhat V, Balakrishnan M, et al. Bioactivity and surface characteristics of titanium implants following various surface treatments: an in vitro study. J Oral Implant. 2014. doi:10.1563/aaid-joi-D-13-00292.
37. Teixeira LN, Crippa GE, Lefebvre LP, et al. The influence of pore size on osteoblast phenotype expression in cultures grown on porous titanium. Int J Oral Maxillofac Surg. 2012;41(9):1097–101.
38. Caparros C, Guillem-Marti J, Molmeneu M, et al. Mechanical properties and in vitro biological response to porous titanium alloys prepared for use in intervertebral implants. J Mech Behav Biomed Mater. 2014;39:79–86.
39. Takemoto M, Fujibayashi S, Neo M, et al. Mechanical properties and osteoconductivity of porous bioactive titanium. Biomaterials. 2005;26(30):6014–23.
40. Carinci F, Pezzetti F, Volinia S, et al. Analysis of MG63 osteoblastic-cell response to a new nanoporous implant surface by means of a microarray technology. Clin Oral Implant Res. 2004;15(2):180–6.
41. Cooper LF, Masuda T, Yliheikkila PK, Felton DA. Generalizations regarding the process and phenomenon of osseointegration. Part II. In vitro studies. Int J Oral Maxillofac Implant. 1998;13(2):163–74.
42. Ferraz EP, Sa JC, de Oliveira PT, et al. The effect of plasma-nitrided titanium surfaces on osteoblastic cell adhesion, proliferation, and differentiation. J Biomed Mater Res A. 2014;102(4):991–8.
43. Capellato P, Smith BS, Popat KC, Alves Claro APR. Fibroblast functionality on novel Ti-30Ta nanotube array. Mater Sci Eng C Mater Biol Appl. 2012;32(7):2060–7.
44. Hofstetter W, Sehr H, de Wild M, et al. Modulation of human osteoblasts by metal surface chemistry. J Biomed Mater Res A. 2013;101(8):2355–64.
45. Hughes FJ, Turner W, Belibasakis G, Martuscelli G. Effects of growth factors and cytokines on osteoblast differentiation. Periodontology. 2000;2006(41):48–72.
46. Hu Y, Tang XX, He HY. Gene expression during induced differentiation of sheep bone marrow mesenchymal stem cells into osteoblasts. Genet Mol Res. 2013;12:6527–34.
47. Pereira KK, Alves OC, Novaes AB, et al. Progression of osteogenic cell cultures grown on microtopographic titanium coated with calcium phosphate and functionalized with a type I collagen-derived peptide. J Periodontol. 2013;84(8):1199–210.
48. de Oliveira PT, Nanci A. Nanotexturing of titanium-based surfaces upregulates expression of bone sialoprotein and osteopontin by cultured osteogenic cells. Biomaterials. 2004;25(3):403–13.
49. Haynes DR, Rogers SD, Hay S, Pearcy MJ, Howie DW. The differences in toxicity and release of bone-resorbing mediators induced by titanium and cobalt-chromium-alloy wear particles. J Bone Joint Surg Am. 1993;75(6):825–34.